surfaces

MDPI

Article

Naringenin Release to Biomembrane Models by Incorporation into Nanoparticles. Experimental Evidence Using Differential Scanning Calorimetry

Cristina Torrisi, Marco Di Guardia, Francesco Castelli and Maria Grazia Sarpietro *

Department of Drug and Health Sciences, University of Catania, Viale Andrea Doria 6, 95125 Catania, Italy; torrisi.cristina@hotmail.it (C.T.); marco.diguardia@hotmail.it (M.D.G.); fcastelli@unict.it (F.C.)
* Correspondence: mg.sarpietro@unict.it; Tel.: +39-0957384260

Abstract: Naringenin (4′,5,7-trihydroxyflavanone-7-rhamnoglucosideor naringenin-7-rhamnoglucoside), a flavonoid present in large quantities in citrus, has different beneficial effects on human health as an antioxidant, free radical scavenger, anti-inflammatory, carbohydrate metabolism promoter, and immune system modulator. Different studies have shown that this substance also has a hypoglycemic and antihypertensive effect, reduces cholesterol and triglycerides, and plays an important protective role in the heart tissue; moreover, it provides neuroprotection against various neurological disorders such as Parkinson's disease and unpredictable chronic stress-induced depression. Despite these advantages, Naringenin is poorly absorbed, and the small percentage absorbed is rapidly degraded by the liver, as a result losing its activity. Several approaches have been attempted to overcome these obstacles, among them, nanotechnology, with the use of Drug Delivery Systems (DDS) as Solid Lipid Nanoparticles (SLN) and Nanostructured Lipid Carriers (NLC). DDS can, in fact, improve the drug bioavailability. The aim of this study was to develop and characterize SLN and NLC containing Naringenin and to evaluate the ability of these nanoparticles to release Naringenin at the cell level using biomembrane models represented by Multilamellar Vesicles (MLV). These studies were performed using Differential Scanning Calorimetry, a powerful technique to detect the interaction of drugs and delivery systems with MLV. It was shown that Naringenin could be better incorporated into NLC with respect to SLN and that Naringenin could be released by NLC into the biomembrane model. Therefore, suggesting the administration of Naringenin loaded into nanoparticles could help avoid the disadvantages associated with the use of the free molecule.

Keywords: Naringenin; differential scanning calorimetry; nanoparticles; multilamellar vesicles; biomembrane model

Citation: Torrisi, C.; Di Guardia, M.; Castelli, F.; Sarpietro, M.G. Naringenin Release to Biomembrane Models by Incorporation into Nanoparticles. Experimental Evidence Using Differential Scanning Calorimetry. *Surfaces* **2021**, *4*, 295–305. https://doi.org/10.3390/surfaces4040025

Academic Editor: Mukhtar H. Ahmed

Received: 26 October 2021
Accepted: 25 November 2021
Published: 29 November 2021

1. Introduction

Naringenin (4′,5,7-trihydroxyflavanone-7-rhamnoglucosideor naringenin-7-rhamnoglucoside, NAR) is a flavonoid present in large quantities in citrus. It is considered as having different bioactive effects on human health as an antioxidant, free radical scavenger, anti-inflammatory, carbohydrate metabolism promoter, and immune system modulator [1,2]. Different in vitro and in vivo studies have shown that this substance also has a hypoglycemic and antihypertensive effect, reduces cholesterol and triglycerides, and plays an important protective role in the heart tissue [3]. Furthermore, other studies have demonstrated that Naringenin provides neuroprotection against various neurological disorders, as in the case of Parkinson's disease [4] and unpredictable chronic stress-induced depression [5]. Reasonably, Naringenin might seem to be the cure for different ills, but some problems have to be considered: the first relates to studies on animals which use doses that cannot be administered to humans; second, this substance is poorly absorbed, and the small percentage absorbed, around 15%, is rapidly degraded by the liver, losing its activity as a result [6]; the third and most significant negative aspect is the inhibitory effect

of the activity of some cytochrome P450 isoforms [7], an enzymatic complex that has a fundamental role in the degradation and elimination of different drugs. However, if the drugs degraded by the cytochrome P450 are taken in conjunction with the ingestion of the grapefruit, the bioactive substances present in the citrus would reduce the enzyme activity and change the bioavailability of the drugs, in addition to causing an overdose or a lack of efficacy which could have serious effects [8]. Various approaches have been proposed to overcome these obstacles, such as cocrystals formation [9], methylation [10], incorporation in delivery systems [11,12], and the synthesis of functionalized lipophilic O-alkyl naringenin derivatives [13]. Solid lipid nanoparticles (SLN) and nanostructured lipid carriers (NLC) are two lipid-based drug delivery systems used in this study. SLN and NLC have been introduced as potential delivery systems due to their high encapsulation ability, control release, and targeting delivery properties that allow a reduction of the total dose of the drug and its side effects [14–16]. In addition, they can protect the drugs against enzymes and can slow down drug degradation and elimination, thereby enhancing the bioavailability of drugs [17]. The aim of this study was to develop and characterize SLN and NLC containing Naringenin. The ability of these nanoparticles to release Naringenin at the cell level was also investigated. The processes involved in SLN and NLC uptake by cells are very complex, and the biomembranes are very complicated structures; as a consequence, the interactions between SLN or NLC and the biomembrane are difficult to study and understand. For this reason, biomimetic model cell membranes are widely used to study such interactions [18]. In this work, as a cell membrane model, we used multilamellar vesicles (MLV) made of dimyristoylphosphatidylcholine (DMPC). The Differential Scanning Calorimetry (DSC) technique was used for this study. DSC, which can reveal the effect of "stranger" molecules on the MLV, is a suitable technique to study the interaction of drugs and lipids and the transfer kinetics of a drug from a drug delivery system to a biomembrane model [19–22]. It was shown that NLC could better incorporate Naringenin with respect to SLN and that Naringenin could be released by NLC into the biomembrane model. These studies suggest that the administration of Naringenin-loaded nanoparticles could prevent the disadvantages associated with the use of the free molecule.

2. Materials and Methods

2.1. Materials

Cethyl palmitate (Cutina, CP), Glyceriloleate (Tegin 0), Oleth-20 and isopropyl myristate were obtained from A.C.E.F. S.p.a (Piacenza, Italy). Naringenin (95% purity), was provided by Sigma-Aldrich (Milan, Italy). Dimyristoylphospatidylcholine (DMPC) was obtained from Genzyme (Liestal, Switzerland).

2.2. SLN and NLC Preparation

Naringenin-loaded SLN (containing 1% and 2% of Naringenin, SLN N 1%, and SLN N 2%, respectively) and Naringenin-loaded NLC (containing 1% and 2% of Naringenin, NLC N 1%, and NLC N 2%, respectively) were prepared by the Phase Inversion Temperature (PIT) method. Unloaded SLN and unloaded NLC were also prepared. The SLN and NLC composition is reported in Table 1. Briefly, the lipid phase consisting of Cutina, Oleth-20, and Tegin O and the aqueous phase were heated at 85–90 °C under stirring. Naringenin was added to the lipid phase at 85 °C. When the two phases reached the same temperature, the aqueous phase was slowly poured into the lipid phase under stirring. The opaque formulation became transparent, realizing the phase inversion from a W/O system to an O/W system. The formulation was taken to room temperature under stirring. Isopropyl Myristate was added as a liquid lipid for the NLC preparation [23].

Table 1. Composition of unloaded SLN, Naringenin-loaded SLN (SLN N1% and SLN N 2%) unloaded NLC and Naringenin loaded NLC (NLC N 1% and NLC N 2%).

Sample	Cetil Palmitate (g)	Tegin O (g)	Oleth-20 (g)	Isopropyl Myristate (g)	Naringenin (g)	H_2O (g)
SLN	1.40	0.880	1.720	-	-	16.000
SLN N 1%	1.40	0.880	1.720	-	0.014	15.986
SLN N 2%	1.40	0.880	1.720	-	0.028	15.930
NLC	1.22	0.772	1.520	0.500	-	15.980
NLC N 1%	1.22	0.772	1.520	0.500	0.012	15.975
NLC N 2%	1.22	0.772	1.520	0.500	0.024	15.927

2.3. Speed Vacuum Drying

Nanoparticle samples were dried by the Speed Vacuum Eppendorf Concentrator plus, a centrifugation system where a pump applied a high vacuum, allowing the elimination of solvents without requiring strong conditions that could destroy the nanoparticles.

2.4. Characterization of Nanoparticles

The particle size and polydispersity index (P.I.) of nanoparticles were measured by Dynamic Light Scattering (DLS), using a Zeta Sizer Nano-ZS90 (Malvern Instrument Ltd., Worcs, UK) equipped with a laser whose nominal power is 4.5 mW with a maximum power of 5 mW at 670 nm. The analyses were performed using a 90° scattering angle at 20 ± 0.2 °C. Before measurements, each sample was diluted in deionized water. Each measurement was repeated three times.

2.5. Stability Tests

To investigate the stability, SLN and NLC samples were stored in a hermetically sealed bottle at room temperature for three months. The particle size and the polydispersity index of the samples were determined after 24 h, a week, and at the end of the 1st, 2nd, and 3rd months.

2.6. Preparation of MLV

MLV were prepared both in the absence and presence of Naringenin. DMPC and Naringenin were separately solubilized in chloroform/methanol (1:1, *V/V*). Aliquots of the DMPC solution (0.010325 mmoles of DMPC) were delivered in glass tubes. An aliquot of the Naringenin solution was added to the glass tubes in order to have a 0.12 molar fraction of Naringenin. MLV without Naringenin were also prepared. The solvents were evaporated under nitrogen flux. Solvent residues were eliminated by freeze-drying. 168 µL of TRIS buffer (hydroxymethyl)-aminomethane 50 mM (pH = 7.4) was added. The samples were kept at 37 °C for 1 min and vortexed for 1 min three times. Finally, the samples were kept at 37 °C for 60 min [24].

2.7. DSC Analysis

Calorimetric analysis was performed using a Mettler Toledo STARe system (Greifensee, Switzerland) equipped with a DSC1 calorimetric cell. A Mettler TA-STARe software (version 16.00) was used to obtain and analyze data. The sensitivity was automatically chosen as the maximum that was possible by the calorimetric system. The calorimeter was calibrated using Indium (99.95% purity). 160 µL aluminum calorimetric pans were used. The reference pan was filled with 120 µL of deionized water.

2.7.1. SLN, NLC, and MLV Calorimetric Analysis

Aliquots of 120 µL of the samples were transferred in 160 µL DSC aluminum pans, hermetically sealed, and subjected to a calorimetric analysis under Nitrogen flow (60 mL/min) as follows: (i) a heating scan from 5 °C to 70 °C, at 2 °C/min, and (ii) a cooling scan from 70 °C to 5 °C, at 4 °C/min, three times to check the reproducibility of the results.

2.7.2. Calorimetric Analysis of Dry Samples

The dry samples were put in the calorimetric pans, hermetically sealed, and subjected to a calorimetric analysis under Nitrogen flow (60 mL/min) as follows: a heating scan from 25 °C to 300 °C, at 2 °C/min.

2.7.3. Naringenin and MLV Contact Kinetic

An exact amount of Naringenin corresponding to a 0.12 molar fraction with respect to the DMPC was weighed on the bottom of the pan, and 120 µL of MLV were added to it. The pan was hermetically sealed and subjected to a calorimetric analysis as follows: a heating scan between 5 and 70 °C at the rate of 2 °C/min; a cooling scan between 70 and 37 °C at the rate of 4 °C/min; an isothermal period (1 h) at 37 °C and a cooling scan between 37 and 5 °C (4 °C/min). This procedure was repeated eight times [25].

2.7.4. SLN/MLV and NLC/MLV Contact Kinetic

90 µL of the MLV dispersion and 30 µL of SLN or NLC (empty or loaded with Naringenin) were placed into the 160 µL pan. The pan was sealed and put into the calorimetric cell. The samples were subjected to a calorimetric analysis as described in "Naringenin and MLV contact kinetic" [26].

3. Results and Discussion

3.1. Nanoparticle Characterization

Unloaded and Naringenin-loaded nanoparticles, prepared by the PIT method, showed small particle sizes. The addition of Naringenin produced a little decrease in the nanoparticle size. P.I. values were around 0.300, suggesting the presence of a homogeneous population of nanoparticles in the investigated samples (Table 2). The average sizes, the polydispersity index, and the calorimetric curves did not show significative differences over time, suggesting that the nanoparticle systems remained stable over the indicated period.

Table 2. The average size and polydispersity index (P.I.) of unloaded SLN, Naringenin-loaded SLN, unloaded NLC, and Naringenin-loaded NLC.

Sample	Size ± SD (nm)	P.I. ± SD
SLN	39.62 ± 0.42	0.287 ± 0.060
SLN N 1%	31.28 ± 1.32	0.350 ± 0.062
SLN N 2%	34.75 ± 0.54	0.304 ± 0.046
NLC	31.94 ± 0.82	0.304 ± 0.034
NLC N 1%	29.10 ± 0.24	0.277 ± 0.054
NLC N 2%	29.93 ± 0.73	0.335 ± 0.043

3.2. DSC Analysis of Nanoparticles

The curves of SLN and NLC subjected to a calorimetric analysis were compared with the curve of Cutin (Figure 1). The calorimetric curves of Cutin, SLN, and NLC are characterized respectively by a main peak at about 54 °C, 45 °C, and 43 °C and a shoulder at a lower temperature. The shift of the peak of SLN and NLC to a lower temperature with respect to Cutin is due to interactions between the lipid and the surfactants which give a less ordered structure [27].

The calorimetric curves of SLN N 1% and SLN N 2% do not show a particular variation with respect to the curve of unloaded SLN; in fact, the temperature and the intensity of the peak remain almost unchanged (Figure 2); instead, Naringenin causes significant variations in the NLC calorimetric curve (Figure 3); in fact, in the presence of 1% Naringenin, the shoulder disappears and the curve shows a single peak at a lower temperature than empty NLC; at 2% of Naringenin, the peak is even lower. Enthalpy values slightly decrease. These results indicate that Naringenin could be distributed homogeneously within the NLC and that it affects the system.

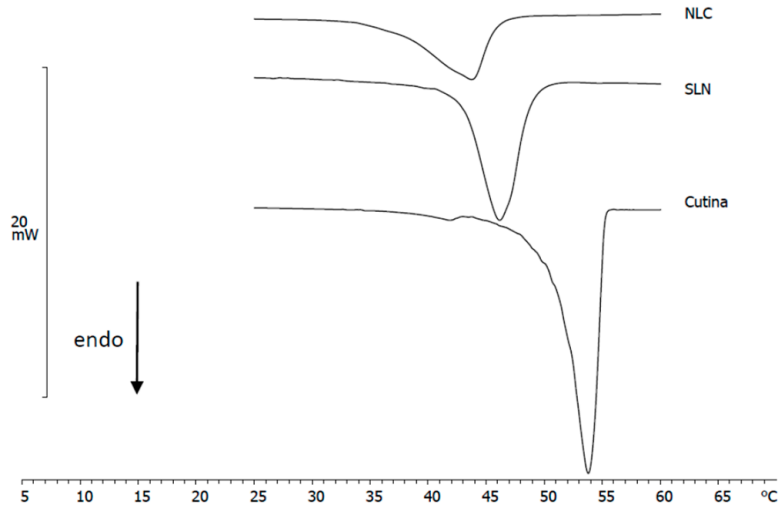

Figure 1. Calorimetric curves, in heating mode, of cutina, SLN, and NLC.

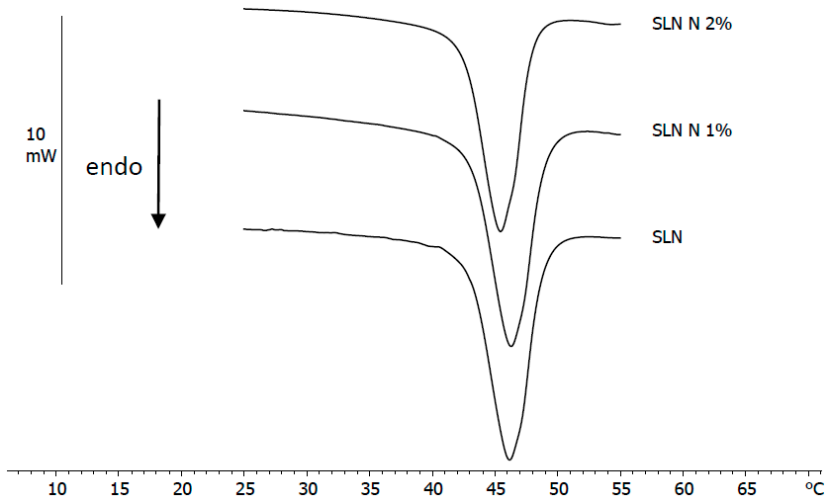

Figure 2. Calorimetric curves, in heating mode, of unloaded SLN, 1% Naringenin-loaded SLN (SLN N 1%), and 2% Naringenin-loaded SLN (SLN N 2%).

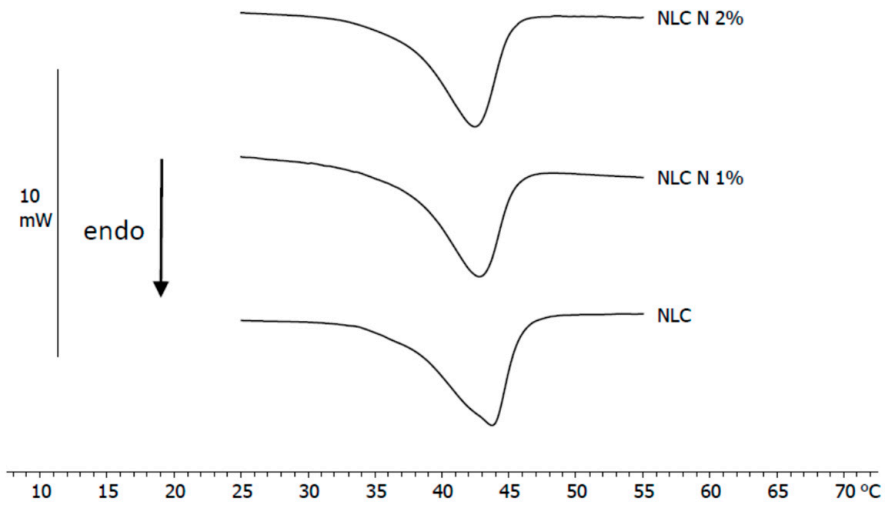

Figure 3. Calorimetric curves, in heating mode, of unloaded NLC, 1% Naringenin-loaded NLC (NLC N 1%), and 2% Naringenin-loaded NLC (NLC N 2%).

3.3. Calorimetric Analysis of Dry Samples

This study was carried out to have information on Naringenin inside the nanoparticles. The dried samples of Naringenin-loaded SLN and Naringenin-loaded NLC were subjected to a calorimetric analysis. Their calorimetric curves (Figure 4) were compared with that of Naringenin. Naringenin shows a melting peak centered at 253.9 °C. The calorimetric curve of Naringenin-loaded SLN shows a peak at 45 °C, as expected, and a small peak at about 254 °C, corresponding to the Naringenin melting peak; in Naringenin-loaded NLC, a single peak at 43 °C is present with no evidence of the peak at 254 °C. These results indicate that Naringenin is mostly located inside the SLN in an amorphous form and that a small part remains outside in a crystalline form. In contrast, Naringenin is completely localized in an amorphous form in the NLC.

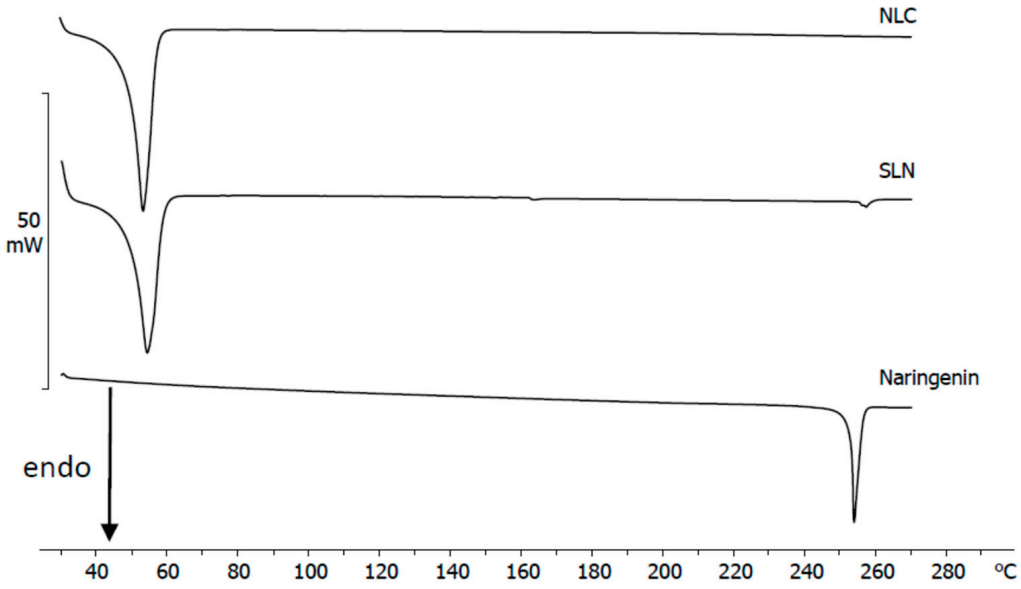

Figure 4. Calorimetric curves, in heating mode, of Naringenin, Naringenin-loaded SLN, and Naringenin-loaded NLC after speed-vacuum drying.

3.4. Naringenin and MLV Contact Kinetic

The DMPC MLV (used as a biomembrane model) calorimetric curve is characterized by a pre-transition peak at around 17 °C (related to the transition from the ordered phase to the ripple phase) and a main transition peak at around 25 °C (related to the transition from the ripple phase to the disordered phase) [28,29]. The interaction of a substance with MLV could cause the change of the pre-transition and/or the main transition peak [30,31]. Naringenin was put in contact with the MLV, and the interaction between Naringenin and MLV, at an increasing time of contact, was investigated by calorimetric analysis. The calorimetric curves were compared with those of the MLV and the MLV prepared with Naringenin at a 0.12 molar fraction (Figure 5). The latter curve is used as a reference; in fact, if Naringenin was absorbed by the phospholipidic bilayers, a calorimetric curve similar to this would be obtained. The disappearance of the pretransition peak and a small decrease in intensity of the main peak are observed. The transition temperature remains almost unchanged. A curve similar to the reference one has never been obtained. These results indicate that only a small amount of Naringenin is absorbed into the MLV.

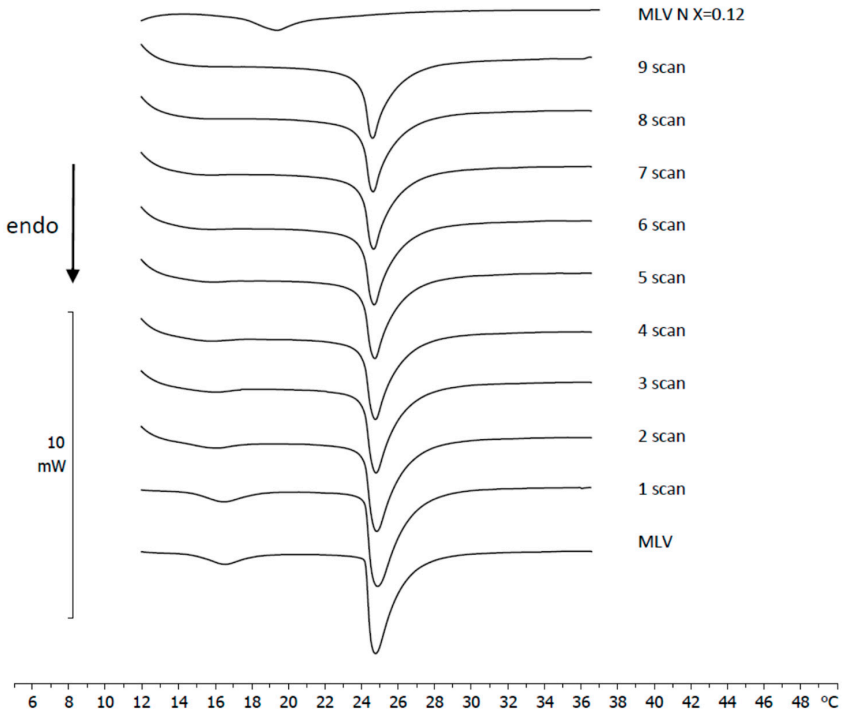

Figure 5. Calorimetric curves, in heating mode, of MLV left in contact with Naringenin (molar fraction 0.12). The calorimetric curves are compared with that of MLV prepared with Naringenin at a 0.12 molar fraction.

3.5. SLN/MLV and NLC/MLV Contact Kinetic

These experiments were carried out to study the eventual interaction between MLV, used as biomembrane model, and SLN or NLC. SLN or NLC were put in contact with MLV and the sample submitted to DSC analysis. The calorimetric curves were compared with the calorimetric curve of the samples analyzed before the contact (MLV and unloaded SLN; MLV and loaded SLN; MLV and unloaded NLC; MLV and loaded NLC) (Figures 6 and 7). If the nanoparticles were able to interact with the biomembrane model, there could be a variation in the calorimetric curve of the samples put in contact. The calorimetric curves of the MLV left in contact with unloaded SLN are shown in Figure 6a; the pre-transition peak of MLV disappears and the main peak gradually decreases while the SLN peak slightly thins. These results indicate that SLN interact with MLV, keeping their structure almost unchanged. In particular, the nanoparticles might be introduced between the phospholipid bilayers of MLV, as indicated by the decrease in intensity of the calorimetric peak. The calorimetric curves of MLV put in contact with SLN N 2% are shown in Figure 6b; also, in this case, the pre-transition peak of MLV disappears and the intensity of the main peak decreases; the peak relative to the SLN N 2% undergoes slight variations. The calorimetric curves of MLV put in contact with unloaded NLC are shown in Figure 7a. The calorimetric peaks related to MLV vary; in fact, the pre-transition peak disappears, while the transition peak becomes gradually smaller. The peak related to NLC gradually broadens. These results indicate that NLC could be able to interact with the biomembrane model, probably by entering their phospholipid bilayers (indicated by the decrease in intensity of the calorimetric peak). The calorimetric curves of the interaction between MLV put in contact with NLC N 2% are shown in Figure 7b: the disappearance of the pre-transition peak and the decrease of the MLV main peak are observed; moreover, the signal related to NLC N 2% broadens; in addition, a small shoulder at a lower temperature (characteristic of empty NLC) appears. This might indicate that NLC go inside the MLV structure and release Naringenin. To obtain more information on the interaction between MLV and nanoparticles that are put in contact at increasing times, the values of the enthalpy

variation (as $\Delta\Delta H/\Delta H^0$; $\Delta\Delta H = \Delta H - \Delta H^0$, where ΔH is the variation of the transition enthalpy of the DMPC MLV in the presence of each system under analysis, and ΔH^0 is the variation of the transition enthalpy of the DMPC MLV) of the MLV transition peak are shown in Figure 8, as a function of the calorimetric scans. In all the systems analyzed, a decrease in the enthalpy variation of MLV occurs. If unloaded SLN and unloaded NLC are compared, it can be noticed that the SLN cause a higher decrease in the enthalpy variation than the NLC; this indicates that SLN can affect the structure of MLV more than NLC. Unloaded and Naringenin-loaded SLN produce a comparable decrease of the enthalpy variation; therefore, the effect is attributed to the SLN; this behavior suggests that SLN, although they can insert themselves into the structure of the biomembrane model, are not able to release Naringenin. The loaded NLC produce a higher decrease of the enthalpy variation than unloaded NLC; this higher effect may be attributed to NLC and to Naringenin. For this reason, it is possible to suppose that NLC enter into the biomembrane model structure and release Naringenin.

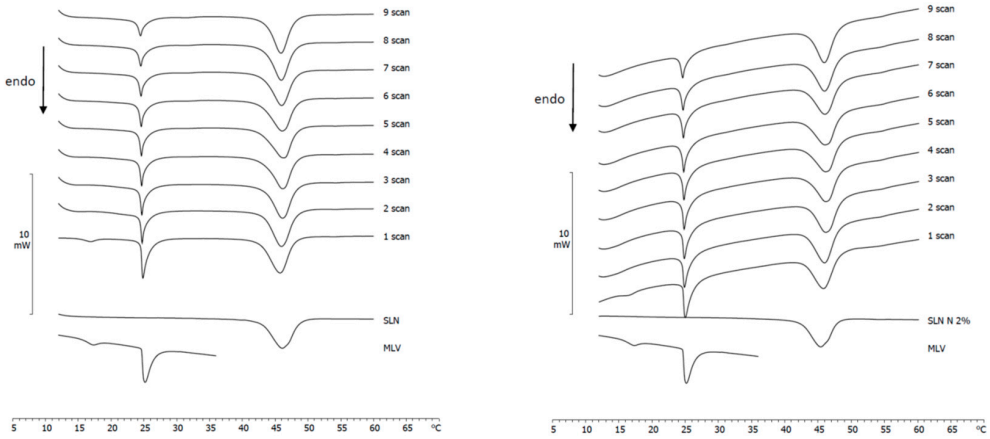

(**a**) (**b**)

Figure 6. (**a**) Calorimetric curves, in heating mode, of MLV left in contact with unloaded SLN. The calorimetric curves are compared with the calorimetric curves of MLV and SLN. (**b**) Calorimetric curves, in heating mode, of MLV left in contact with 2% Naringein-loaded SLN. The calorimetric curves are compared with the calorimetric curves of MLV and 2% Naringenin-loaded SLN.

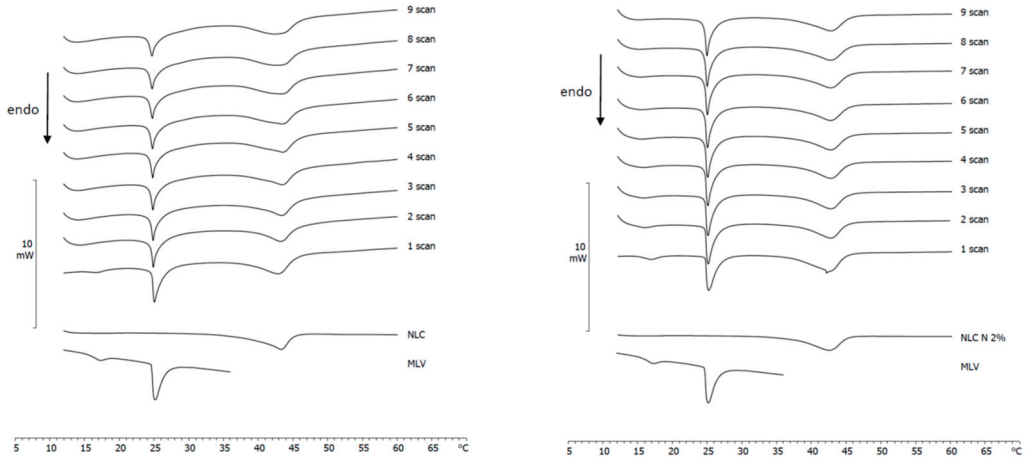

(**a**) (**b**)

Figure 7. (**a**) Calorimetric curves, in heating mode, of MLV left in contact with unloaded NLC. The calorimetric curves are compared with the calorimetric curves of MLV and NLC. (**b**) Calorimetric curves, in heating mode, of MLV left in contact with 2% Naringein-loaded NLC. The calorimetric curves are compared with the calorimetric curves of MLV and 2% Naringenin-loaded NLC.

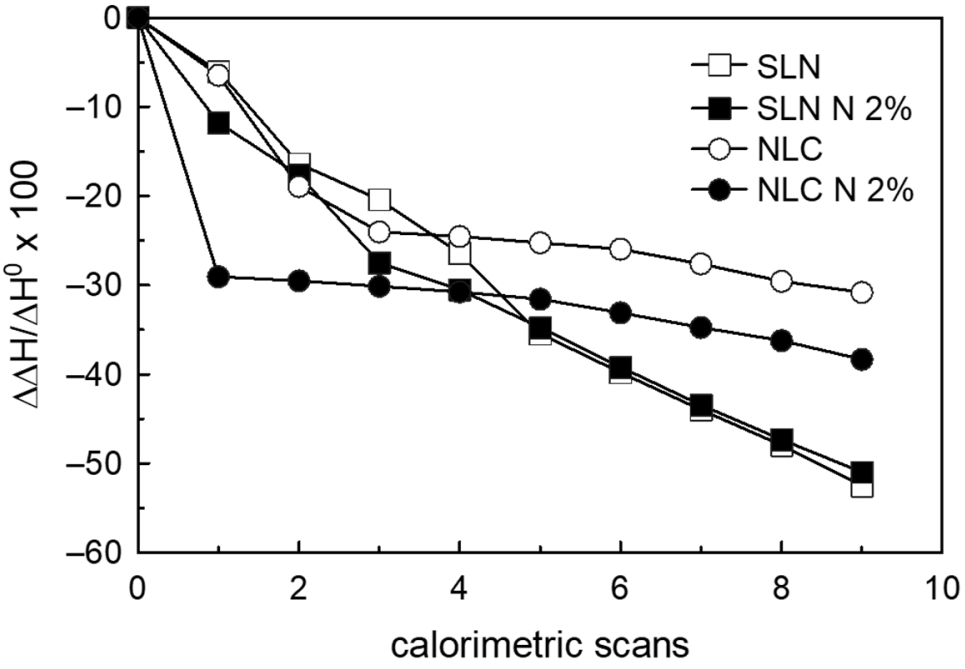

Figure 8. Transition enthalpy variation of MLV left in contact with unloaded SLN, 2% Naringenin-loaded SLN, unloaded NLC, and 2% Naringenin-loaded NLC, as a function of the calorimetric scans. The transition enthalpy variation is reported as $\Delta\Delta H/\Delta H^0$ ($\Delta\Delta H = \Delta H - \Delta H^0$, where ΔH is the transition enthalpy variation of the MLV left in contact with SLN or NLC, and ΔH^0 is the transition enthalpy variation of MLV).

4. Conclusions

Naringenin is an interesting compound with promising activities in the pharmacological field. Despite its activities, it is often not used because it is poorly absorbed. To overcome this obstacle, Naringenin can be encapsulated in nanoparticles. Loaded-Naringenin SLN and NLC were prepared by the PIT method. The ability of SLN and NLC to delivery Naringenin was evaluated by using the DSC technique and multilamellar vesicles of DMPC representing a biomembrane model. The DSC permitted one to study (1) the interaction between the lipid matrix and Naringenin and (2) the diffusion of Naringenin from the nanocarriers to the biomembrane model. The calorimetric results indicate that Naringenin interacts with the nanocarriers and suggest their potential use as delivery systems for this compound. The incorporation of Naringenin into nanocarriers would allow for its oral administration, thus protecting the molecule against enzymatic degradation.

Author Contributions: Conceptualization, F.C. and M.G.S.; methodology, M.G.S.; software, C.T. and M.D.G.; validation, C.T. and M.D.G.; formal analysis, C.T. and M.D.G.; investigation, F.C.; resources, F.C. and M.G.S.; data curation, C.T., M.D.G. and M.G.S.; writing—original draft preparation, M.D.G. and M.G.S.; writing—review and editing, M.G.S. and F.C.; supervision, M.G.S.; project administration, M.G.S. All authors have read and agreed to the published version of the manuscript.

Funding: This research received no external funding.

Institutional Review Board Statement: Not applicable.

Informed Consent Statement: Not applicable.

Data Availability Statement: Data is available on request from the corresponding author.

Conflicts of Interest: The authors declare no conflict of interest.

References

1. Felgines, C.; Texier, O.; Morand, C.; Manach, C.; Scalbert, A.; Régerat, F.; Rémésy, C. Bioavailability of the flavanone naringenin and its glycosides in rats. *Am. J. Physiol. Gastrointest. Liver Physiol.* **2000**, *27*, G1148–G1154. [CrossRef] [PubMed]
2. Jeon, S.M.; Kim, H.K.; Kim, H.J.; Do, G.M.; Jeong, T.S.; Park, Y.B.; Choi, M.S. Hypocholesterolemic and antioxidative effects of naringenin and its two metabolites in high-cholesterol fed rats. *Transl. Res.* **2007**, *149*, 15–21. [CrossRef]
3. Ashraful, A.M.; Nusrat, S.; Mahbubur, R.M.; Shaikh, J.U.; Hasan, M.R.; Satyajit, D. Effect of citrus flavonoids, naringin and naringenin, on metabolic syndrome and their mechanisms of action. *Adv. Nutr.* **2014**, *5*, 404–417.
4. Chen, C.; Wei, Y.Z.; He, X.M.; Li, D.D.; Wang, G.Q.; Li, J.J.; Zhang, F. Naringenin produces neuroprotection against lps-induced dopamine neurotoxicity via the inhibition of microglial NLRP3 inflammasome activation. *Front. Immunol.* **2019**, *10*, 936. [CrossRef]
5. Tayyab, M.; Farheen, S.M.; Khanam, N.; Hossain, M.M.; Shahi, M.H. Antidepressant and neuroprotective effects of naringenin via sonic hedgehog-gli1 cell signaling pathway in a rat model of chronic unpredictable mild stress. *Neuromol. Med.* **2019**, *21*, 250–261. [CrossRef] [PubMed]
6. Dow, C.; Going, S.; Chow, H.-H.; Patil, B.; Thomson, C. The effect of daily consumption of grapefruit on body weight, lipids, and blood pressure in healthy, overweight adults. *Metab. Clin. Exp.* **2012**, *61*, 1026–1035. [CrossRef] [PubMed]
7. Bailey, D.G.; Malcolm, J.; Arnold, O.; Spence, J.D. Grapefruit juice–drug interactions. *Br. J. Clin. Pharmacol.* **1998**, *46*, 101–110. [CrossRef]
8. Bressler, R. Grapefruit juice and drug interactions. Exploring mechanisms of this interaction and potential toxicity for certain drugs. *Geriatrics* **2006**, *61*, 12–18.
9. Cui, W.; He, Z.; Zhang, Y.; Fan, Q.; Feng, N. Naringenin cocrystals prepared by solution crystallization method for improving bioavailability and anti-hyperlipidemia effects. *AAPS PharmSciTech* **2019**, *20*, 115. [CrossRef]
10. Copmans, D.; Orellana-Paucar, A.M.; Steurs, G.; Zhang, Y.; Ny, A.; Foubert, K.; Exarchou, V.; Siekierska, A.; Kim, Y.; De Borggraeve, W.; et al. Methylated flavonoids as anti-seizure agents: Naringenin 4′, 7-dimethyl ether attenuates epileptic seizures in zebrafish and mouse models. *Neurochem. Int.* **2018**, *112*, 124–133. [CrossRef]
11. Wang, Y.; Wang, S.; Firempong, C.K.; Zhang, H.; Wang, M.; Zhang, Y.; Zhu, Y.; Yu, J.; Xu, X. Enhanced solubility and bioavailability of naringenin via liposomal nanoformulation: Preparation and in vitro and in vivo evaluations. *AAPS PharmSciTech* **2017**, *18*, 3. [CrossRef] [PubMed]
12. Bhia, M.; Motallebi, M.; Abadi, B.; Zarepour, A.; Pereira-Silva, M.; Saremnejad, F.; Santos, A.C.; Zarrabi, A.; Melero, A.; Jafari, S.M.; et al. Naringenin Nano-Delivery Systems and Their Therapeutic Applications. *Pharmaceutics* **2021**, *13*, 291. [CrossRef] [PubMed]
13. Albuquerque de Oliveira Mendes, L.; Sousa Ponciano, C.; Depieri Cataneo, A.H.; Fanini Wowk, P.; Bordignon, J.; Silva, H.; Vieira de Almeida, M.; Pereira Avila, E. The anti-Zika virus and anti-tumoral activity of the citrus flavanone lipophilic naringenin-based compounds. *Chem.-Biol. Int.* **2020**, *331*, 109218. [CrossRef]
14. Mehnert, W.; Mader, K. Solid Lipid Nanoparticle; production, characterization and applications. *Avd. Drug Deliv. Rev.* **2001**, *2–3*, 165–196. [CrossRef]
15. Radtke, M. Nanostructured lipid carriers. a novel generation of solid lipid drug carriers. *Pharm. Technol. Eur.* **2005**, *17*, 45–50.
16. Mishra, V.; Bansal, K.K.; Verma, A.; Yadav, N.; Thakur, S.; Sudhakar, K.; Rosenholm, J.M. Emerging colloidal nano drug delivery systems. *Pharmaceutics* **2018**, *10*, 191. [CrossRef]
17. Li, Q.; Cai, T.; Huang, Y.; Xia, X.; Cole, S.P.C.; Cai, Y. A review of the structure, preparation, and application of NLCs, PNPs, and PLNs. *Nanomaterials* **2017**, *7*, 122. [CrossRef]
18. Wisniewska-Becker, A.; Gruszecki, W.I. Biomembrane models. In *Drug-Biomebrane Interaction Studies*; The Application of Calorimetric Techniques; Pignatello, R., Ed.; Woodhead Publishing Limited: Cambridge, UK, 2013; pp. 46–95.
19. Castelli, F.; Sarpietro, M.G.; Micieli, D.; Ottimo, S.; Pitarresi, G.; Tripodo, G.; Carlisi, B.; Giammona, G. Differential Scanning Calorimetry Study on Drug Release from an Inulin-based Hydrogel and its Interaction with a Biomembrane Model: pH and Loading Effect. *Eur. J. Pharm. Sci.* **2008**, *35*, 76–85. [CrossRef]
20. Sarpietro, M.G.; Torrisi, C.; Di Sotto, A.; Castelli, F. Interaction of limonene, terpineol, and 1,8 cineol with a model of biomembrane: A DSC study. *Thermochim. Acta* **2021**, *700*, 178938. [CrossRef]
21. Pignatello, R.; Musumeci, T.; Basile, L.; Carbone, C.; Puglisi, G. Biomembrane models and drug-biomembrane interaction studies: Involvement in drug design and development. *J. Pharm. Bioallied Sci.* **2011**, *3*, 4–14. [CrossRef]
22. Chiu, M.H.; Prenner, E.J. Differential scanning calorimetry: An invaluable tool for a detailed thermodynamic characterization of macromolecules and their interactions. *J. Pharm. Bioallied Sci.* **2011**, *3*, 39–59. [PubMed]
23. Montenegro, L.; Sarpietro, M.G.; Ottimo, S.; Puglisi, G.; Castelli, F. Differential scanning calorimetry studies on sunscreen loaded solid lipid nanoparticles prepared by the phase inversion temperature method. *Int. J. Pharm.* **2011**, *415*, 301–306. [CrossRef]
24. Berrio Escobar, J.F.; Pastrana Restrepo, M.H.; Márquez Fernández, D.M.; Martínez Martínez, A.; Giordani, C.; Castelli, F.; Sarpietro, M.G. Synthesis and interaction of sterol-uridine conjugate with DMPC liposomes studied by differential scanning calorimetry. *Colloids Surf. B Biointerfaces* **2018**, *166*, 203–209. [CrossRef]
25. Librando, V.; Accolla, M.L.; Minniti, Z.; Pappalardo, M.; Castelli, F.; Cascio, O.; Sarpietro, M.G. Calorimetric evidence of interaction of brominated flame retardants with membrane model. *Environ. Toxicol. Pharm.* **2015**, *39*, 1154–1160. [CrossRef]
26. Montenegro, L.; Ottimo, S.; Puglisi, G.; Castelli, F.; Sarpietro, M.G. Idebenone loaded solid lipid nanoparticles interact with biomembrane models: Calorimetric evidence. *Mol. Pharm.* **2012**, *9*, 2534–2541. [CrossRef] [PubMed]

27. Siekmann, B.; Westesen, K. Thermoanalysis of the recrystallization process of melt-homogenized glyceride nanoparticles. *Colloids Surf. B Biointerfaces* **1994**, *3*, 159–175. [CrossRef]
28. Koynova, R.; Caffrey, M. Phases and phase transitions of the phosphatidylcholines. *Biochim. Biophys. Acta* **1998**, *1376*, 91–145. [CrossRef]
29. Walde, P. Preparation of vesicles (liposomes). In *ASP Encyclopedia of Nanoscience and Nanotechnology*; Nalwa, H.S., Ed.; American Scientific Publishers: Stevenson Ranch, CA, USA, 2004; Volume 9, pp. 43–79.
30. Jørgensen, K.; Ipsen, J.H.; Mouritsen, O.G.; Bennett, D.; Zuckermann, M.J. A general model for the interactionof foreign molecules with lipid membranes: Drugs andanaesthetics. *Biochim. Biophys. Acta* **1991**, *1062*, 227–238. [CrossRef]
31. Jørgensen, K.; Ipsen, J.H.; Mouritsen, O.G.; Bennett, D.; Zuckermann, M.J. The effects of density fluctuationson the partitioning of foreign molecules into lipid bilayers:application to anaesthetics and insecticides. *Biochim. Biophys. Acta* **1991**, *1067*, 241–253. [CrossRef]